Cumhuriyet Üniversitesi Fen Fakültesi
Fen Bilimleri Dergisi (CFD), Cilt:36, No: 4 Özel Sayı (2015)
ISSN: 1300-1949

Cumhuriyet University Faculty of Science
Science Journal (CSJ), Vol. 36, No: 4 Special Issue (2015)
ISSN: 1300-1949

The influence of crevice volumes on HC pollutants in internal combustion engines

Meysam KALANTARİ[1], Hossein GHOMASHİ[1]

1Department of Mechanical Engineering, South Tehran Branch, Islammic Azad university, Tehran, Iran

Received: 22.03.2015; Accepted: 29.05.2015

Abstract. In the present work, the effect of various parameters on formation of HC pollutants (unburned hydrocarbons) which occurs due to their transition into grooves and crevices of the combustion engine in a light diesel engine was investigated. Numerical calculations for simulation of the combustion chamber were carried out by means of a kind of CFD software called AVL Fire. The computational network field comprised crevice-bearing regions on the cylinder that allowed studying quantity and quality of entities entered the crevices. The effects of crevices and regions among the wall and the cylinder on formation of HC pollutants under different fuel injection methods at basic diesel engines were studied. Single-injection at different times as well as various fuel amounts formed the fuel injection configuration. Formation of HC pollutants occurs after ignition completion and before expansion commencement. It was observed that the highest amount of HC was formed using a retarded fuel injection timetable. At two-step injection, when frequency was increased and injection commenced sooner (advance), formation of HC pollutants was observed to be reduced. Dual injection with small frequency and retarded commencement also led to a significant reduction in HC pollutants formation.

Keywords: Unburned hydrocarbons (HC), Dual injection, Diesel engine, Combustion chamber

1. INTODUCTION

Since their invention, internal combustion engines have undergone a great deal of modifications due to huge developments in technology and human knowledge. Currently, lack of prevailing fuels and increase of environmental limitations have made researchers to find a way to modify and optimize ICE's performance. As a powerful method, computational simulation has invariably challenged its associated processes. Analysis of combustion theories was made possibleby emersion of computers. During the last thirty years improvements in processing ability of computers on one hand and development of our knowledge about physical and chemical reactions on another have surprisingly enhanced achievements in computational modeling.

Krieger and Borman employed a single-zonethermodynamic model to analyze release of energy in a compression ignition engine with direct injection [1]. They assumed that fuel would instantly combine in the cylinder and burn. Obviously, this model is not capable of considering inhomogeneous physical properties of components inside the cylinder. Possible errors in measured pressure data (in terms of amount or phase) affect modeling results. Lyn improved the single-zone thermodynamic model for compression ignition engines [2]. Burning rate of fuel is calculated by an arbitrary (assumed) function which is proportionate to fuel injection rate. Pressure inside the cylinder is obtained by means of heat release rate and thermodynamic analysis.Arbitrary function to calculate combustion rate and an assumption on homogeneity of components inside the cylinder in thermodynamic analysis are known as major blind spots in these models. Karim and Watson developed a single-zone thermodynamic model with chemical kinetics details for H_2O_2 system to investigate auto-ignition under engine modes [3]. In their model, an approximation was proposed to predict energy release rate alterations and chemical species concentrations against time at compression, combustion and expansion stages. The main

* Corresponding author. *Email: Kalantari @gmail.com*

Special Issue: Technological Advances of Engineering Sciences

issue in zero dimensional modeling is that inhomogeneous physical properties of components inside the cylinder may be assumed negligible during a combustion process. Application of such models in exhausting pollutants analysis is utterly limited. Karim and Gao developed a double-zone model to estimate knocking start time and efficiency in a spark ignition engine with methane. In this model, all components inside the cylinder are divided into two zones of burned and unburned by a thin film of flame front [4].Karim and Zhaoda developed a double-zone combustion model to estimate auto-ignition and knocking start points in a compression ignition engine with dual fuel [5]. In this model, the major zone consists of a gas combination of air and fuel and the minor zone is created due to injection and combustion of a little diesel duel. Heat release rate due to chemical reactions in the major zone is obtained by the chemical kinetics method for air-methane combustion reaction. Afterwards, Liu and Karim further developed this double-zone quasi-equilibrium including more details from the chemical kinetics model [6]. Delay in diesel fuel ignition is approximated through an empirical equation proposed by Hiroyasu and Arai [7]. Hiroyasu et al. has also suggested a multi-zone model in which the injected fuel into the cylinder is supposedly divided into 250 divisions with no intervention [8]. Each division consists of air and a set of fuel liquid drops and vapor. The empirical equations of injection penetration and cone angle obtained from combustion experiments in a constant volume bomb are used to determine fuel injection structure in a compression ignition engine. Multi-dimensional modeling of motion inside a cylinder in absence of combustion began in early 1970. Watkins introduced a finite difference method based on simple two-dimensional calculations algorithm for laminar flow, axial symmetry and no combustion in a closed chamber (cylinder) [9]. Following this work, Gausman implemented a method named energy emission for simulation of turbulent flow which was proposed by Jones and Launder [10]. According to the implicit method to solve fluid flow problem at all flow velocities using an arbitrary calculated mesh based on Lagrangian-Eulerian approach to express moving and curve boundaries, Butler developed a computer program which enabled two-dimensionally simulation ofinjection combination processes and combustion in ainjection-guided direct-injected engine [11].

In the present work, the effect of various parameters on formation of HC pollutants which occurs due to their transition into furrows and crevices of the combustion engine in a light diesel engine was investigated. The effects of crevices and regions among the wall and the cylinder on formation of HC pollutants under different fuel injection methods at basic diesel engines were studied. Single-injection at different times as well as various fuel amounts formed the fuel injection configuration.

2. BASIC EQUATIONS AND PATTERNS APPLIED IN SIMULATION

In order to simulate a crevice inside the cylinder, the space between the piston, the cylinder and the crevice related to the first ring including crevice and the seating part was meshed. The distance between the piston and the cylinder wall was 0.335 mm which may be considered as a crevice in the combustion chamber. The sample model is illustrated in figure 1 and compared with a no crevice-bearing model. The equations of mass, momentum and continuity were to be solved for all nodes of this mesh; therefore, mesh size in these areas was considered much finer that other areas of the piston to correctly prediction of transited mass into the crevice.

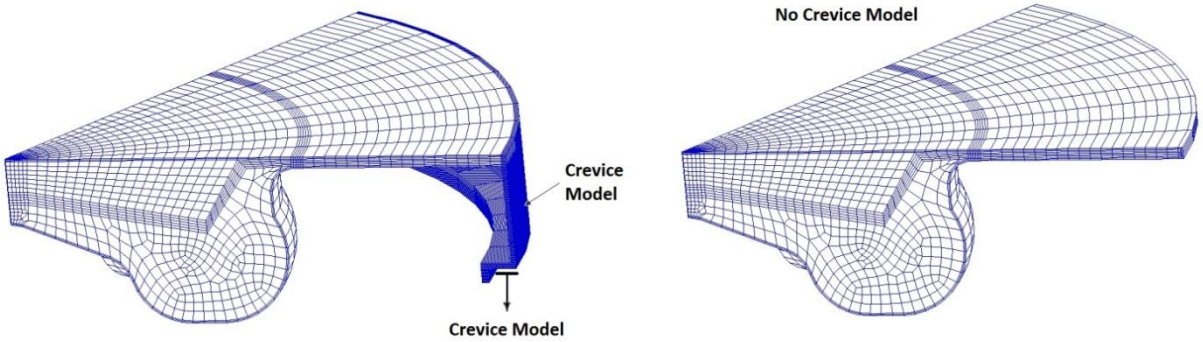

Figure 1. The meshed piston cylinder model.

As may be observed in figure 1, fuel injection line areas, near to the wall and cylinder crevice, are meshed more finely. Mesh numbers when drive shaft was in 360 degrees state (fully closed) was 46670 and when the shaft was put to 180 degrees (fully open) there were 75675 meshes. Nomenclature and different types of boundary layers for the sample model is shown in figure 2.

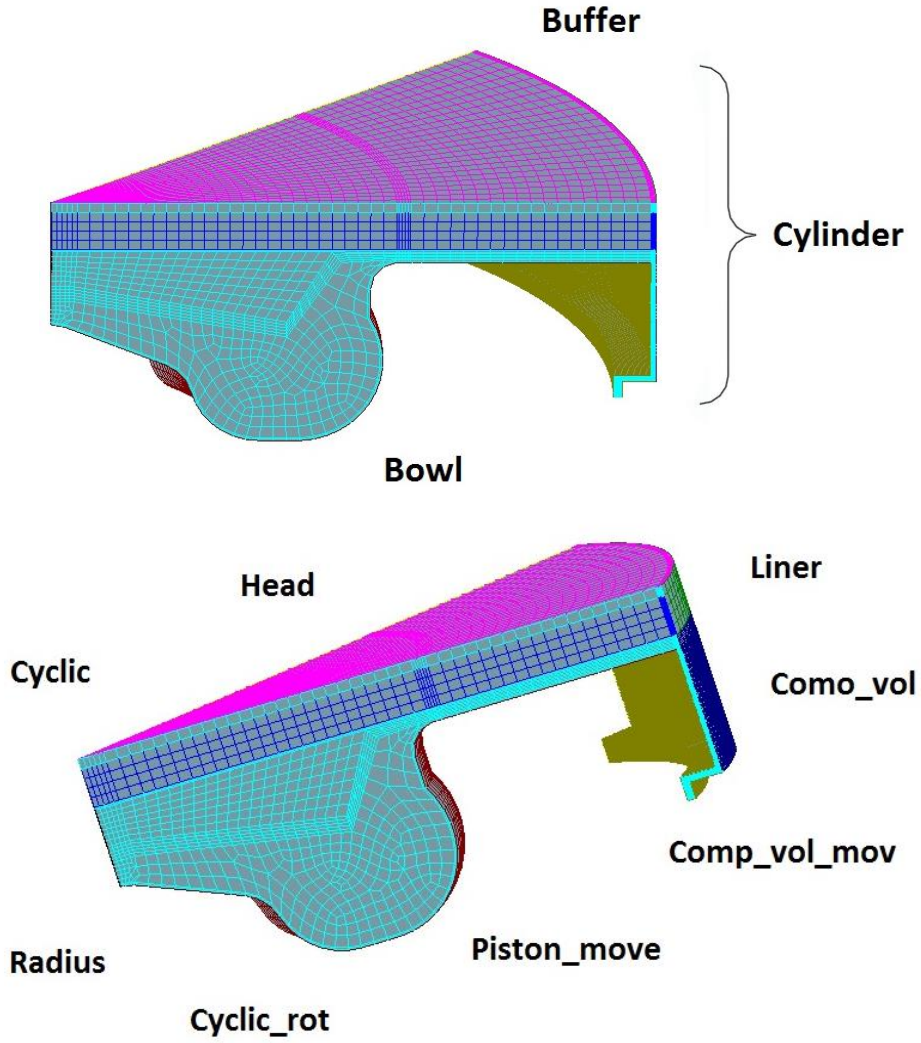

Figure 2. Boundary layers for a: internal and b: surface meshes.

Number and conditions of boundary layers for surface meshes are briefly given in Table 1:

Table 1. Boundary conditions for the sample model.

Head	Boundary layer type: velocity=0; thermal status: T= 553°K
Liner	Boundary layer type: velocity=0; thermal status: T= 403°K
Piston_mov	Boundary layer type: mesh motion; thermal status: T= 593°K
Comp_vol	Boundary layer type: velocity=0; thermal status: Heat flux
Comp_vol_mov	Boundary layer type: velocity=0; thermal status: Heat flux
Cyclic &Cyclic_rot	Boundary layer type: mass transfer (periodic)
Radius	Boundary layer type: Symmetry plane (normal component is velocity and other variables derivations are zero)

2.1. Turbulent flow pattern

The RNG k-ε two-equation turbulence model was used to simulate the turbulent flow inside chamber. Turbulence equations are solved in conjunction with continuity and momentum equationsin order to numerical study of fluid flow.k-ε turbulence equations are:

$$\rho\frac{DK}{Dt} = p - \rho_{\varepsilon} + \frac{\partial}{\partial_{xi}}(\mu\sigma_k\frac{\partial k}{\partial_{xj}}) \quad (1)$$

$$\rho\frac{D\varepsilon}{Dt} = \frac{\varepsilon}{k}(C_{\epsilon 1}\rho - C_{\epsilon 2}\rho\epsilon) - \rho R + C_{\epsilon 3}\rho\epsilon\nabla.u + \frac{\partial}{\partial_{xi}}(\mu\sigma_{\varepsilon}\frac{\partial_{\varepsilon}}{\partial_{xj}}) \quad (2)$$

Where K is kinetic energy of turbulence, ε is rate of kinetic energy loss and p is production of energy which is obtained by the following formula:

$$p = 2C_{\mu}\rho\frac{k^2}{\varepsilon}\left[S_{ij}S_{ij} - \frac{1}{3}(\nabla.U)^2\right] - \frac{2}{3}\rho k\nabla.U \quad (3)$$

Empirical coefficients of the standard k-ε model in above equations are given in Table 2.

Table 2. Determination of coefficients of the standard k-ε turbulent flow pattern.

$C_{\epsilon 1}$	$C_{\epsilon 2}$	$C_{\epsilon 3}$	σ_k	R	C_{μ}
1.68	1.44	-1	0.77	0	0.09

Meanwhile, the term R added to the ε equation in RNG model which has modified this equation is defined as follows:

$$R = \frac{C_{\mu}\rho\eta^3\left(1-\frac{\eta}{\eta_0}\right)}{1+\beta\eta^3}\frac{\varepsilon^2}{k} \quad (4)$$

And also there is:

$$C_{\eta} = \frac{\eta\left(1-\frac{\eta}{\eta_0}\right)}{1+\beta\eta^3} \quad (5)$$

$$C\varepsilon_{RNG} = \frac{-1+2C_{\epsilon 1}-3m_1(n_1-1)+(-1)^{\gamma}\sqrt{k}C_nC_{\eta}\eta}{3} \quad (6)$$

Empirical coefficients of RNG k-ε model are given in Table 3 [12].

Table 3. Determination of empirical coefficients of RNG k-ε turbulent flow patterns.

$C_{\in 1}$	$C_{\in 2}$	$\alpha_k = \alpha_2$	C_μ	η	η_0	β
1.42	1.68	1.39	0.084	$3k/\varepsilon$	4.38	0.012

2.2. Simulation of fuel injection speed through a nozzle

Inlet radius (R) and nozzle length which are determined by inlet parameters, C_1 and C_2, affect effective discharge coefficient [13].

$$C_1 = \frac{R}{D} \quad , \quad C_2 = \frac{L}{D} \tag{7}$$

Inlet pressure, P_1, is obtained by the following formula:

$$P_1 = P_2 + \frac{\rho}{2}.\left(\frac{U_{geo}}{C_d}\right)^2 \tag{8}$$

By means of laminar flow theory and Norwick Theory about calculation of contraction coefficient, C_c, velocity at point c may be calculated from equation of continuity:

$$U_c = \frac{U_{geo}}{C_c} \tag{9}$$

U_{geo} is the theoretical velocity for the laminar flow in nozzle's injector aperture which shows a constant velocity profile. If Bernoulli equation was written for points from 1 to c, with neglecting losses, there would be:

$$P_c = P_1 - \frac{\rho}{2}.U_c^2 \tag{10}$$

When P_c is less that P_{vapor}, the flow may be assumed completely cavitated and new inlet pressure and discharge coefficient may be obtained using the following formulas:

$$P_1 = P_{vapor} - \frac{\rho}{2}.U_c^2 \tag{11}$$

$$C_d = C_c.\sqrt{K} = C_c.\sqrt{\frac{P - P_{vapor}}{P_1 - P_2}} \tag{12}$$

New affecting conditions (nozzle outlet velocity, diameter and area) may be calculated by:

$$U_{eff} = U_c - \frac{P_2 - P_{vapor}}{\rho_1.U_{geo}} \tag{13}$$

$$A_{eff} = A_{geo}.\frac{U_{geo}}{U_{eff}} \tag{14}$$

$$D_{eff} = \sqrt{\frac{4.A_{eff}}{\pi}} \tag{15}$$

Where, C_1 and C_2 are ratios of inlet radius and nozzle's length to its geometric diameter, respectively.

2.3. Combustion pattern

Eddy Breakup combustion models were employed in this work to perform diesel combustion simulations [14].

Average mass fraction rate of fuel:

$$\overline{\omega_p} = \bar{\rho} A \overline{Y_F} \frac{\varepsilon}{k} \tag{16}$$

Average mass fraction rate of oxidizer:

$$\overline{\omega_{O_2}} = \bar{\rho} \frac{A\overline{Y_{O_2}}}{\nu} \frac{\varepsilon}{k} \tag{17}$$

Average mass fraction rate of product:

$$\overline{\omega_p} = \bar{\rho} \frac{A.B}{(1+\nu)} \overline{Y_p} \frac{\varepsilon}{k} \tag{18}$$

2.4. Nitrogen oxide formation pattern

An improved form of Zeldovich mechanism was used in AVL Fire for NO formation kinetics. This mechanism consists of the following equations proposed by Bowman [15]:

$$N_2 + O \overset{k_{1f}}{\underset{k_{1b}}{\leftrightarrow}} NO + N \tag{19}$$

$$N + O_2 \overset{k_{2f}}{\underset{k_{2b}}{\leftrightarrow}} NO + O \tag{20}$$

$$N + OH \overset{k_{3f}}{\underset{k_{3b}}{\leftrightarrow}} NO + H \tag{21}$$

And this relation exists for hydrogen radicals:

$$O + OH \overset{k_{4f}}{\underset{k_{4b}}{\leftrightarrow}} O_2 + H \tag{22}$$

With steady-state assumption for N in above equations, one can obtain:

$$\frac{d}{dt}[NO] = 2k_{1f}[O] + [NO]\left\{\frac{1 - [NO]^2/k_{1f}[O_2][N_2]}{1 + k_{1b}[NO]/(k_{2f}[O_2] + k_{3f}[OH])}\right\} \tag{23}$$

In which, $k_{12} = (\frac{k_{1f}}{k_{1b}})(\frac{k_{2f}}{k_{2b}})$. It is assumed that O, OH, O_2 and N_2 are in thermodynamic equilibrium. NO formation rate constants may be calculated from Arrhenius equation by empirical coefficients.

$$k_f = ATexp\left(\frac{-E_a}{RT}\right) \tag{24}$$

2.5. Soot formation pattern

The used model in Fire code to calculate soot amount includes two stages of soot formation and its oxidation. The overall produced soot may be obtained by subtraction of these stages. Soot formation rate was modeled by Hiroyasu in the following form [16]:

$$\frac{d(M_s)}{dt} = \dot{M_{sf}} - \dot{M_{so}} \tag{25}$$

Where M_S is final soot mass, M_{SF} is soot formation rate and M_{SO} is soot oxidation rate. Arrhenius formation rate of the soot is proportionate to the fuel vapor mass. Hence:

$$\dot{M_{sf}} = k_f M_{fv} \tag{26}$$

$k_f$in above equation is soot formation coefficient which is a function of pressure and temperature and defined as follows:

$$k_f = A_{sf}P^{0.5}exp\left(\frac{-E_{sf}}{RT}\right) \tag{27}$$

Soot oxidation rate is calculated by Nagle/Strickland-Constable model:

$$\dot{M_{so}} = k_O M_s \tag{28}$$

Oxidation coefficient as a function of pressure, temperature and oxygen molar fraction is presented in Equation 29:

$$k_O = A_{so}X_{O_2}P_{1.8}exp\left(\frac{-E_{so}}{RT}\right) \tag{29}$$

Hiroyasu single-step two-process model is schematically illustrated and as it may be observed fuel initially transforms into soot and then into products.

$$Fuel \overset{k_f}{\rightarrow} soot \overset{k_O}{\rightarrow} CO \tag{30}$$

An improved form of that model was used in the employed code. So that, Arrhenius oxidation rate equation was substituted for Nagle/Strickland-Constable oxidation rate which is empirical. In this case, based on experimental results obtained from graphite oxidation in oxygen atmosphere at a given partial pressure range; oxidation rate is modeled through the two mechanisms which are dependent on A and B chemical levels. A levels are highly reactive while B ones have slight reactivity. According to the presented definitions, the rate of oxidation rate in equation 29 is replaced by:

$$k_O = \frac{6}{\rho_s D_{nom}} \dot{W}^n_{asc} \tag{31}$$

Where $\dot{W}^n_{asc}$ is soot oxidation rate per unit area, D_{nom} is the nominal size of soot spherical particles, 25mm and ρ_s is soot density, 2.5 gcm^{-3}.

3. SIMULATION OF SAMPLE MODEL

In order to provide the importing mesh geometry for AVL Fire, GAMBIT 2.0.4 software was used. It is necessary to provide the mesh near the wall in a form so that the first element in adjacent to the wall equals $y^+ \approx 1$ [11].

$$y^+ = \frac{r u_t y}{m} \tag{32}$$

Where $u_t = \sqrt{t_w / r}$ and y is normal distance from the wall.
Simulation in this study was carried out on a sample engine, specifications of which are given in table 4. Engine velocity was constant, 1600 $rev.min^{-1}$ and simulation was performed in a closed cycle i.e. from closure of inlet valve till opening of outlet valve. Areas among the cylinder and the piston as well as the first ring position were considered as crevices. These areas inside the combustion chamber act as suitable places for fuel to be collected and survive oxidation; as a result, soot and unburned HC pollutant are formed. Around 80 per cents of pollutants formed in liner enter engine chamber and the rest are exhausted to the air [17].

Table 4. Specifications of the sample engine [17].

Engine	Light diesel
Cylinder head	Flat
Cylinder displacement (L)	0.5
Compression ratio	18.2
Course length (cm)	8.6
Diameter (cm)	8.6
Piston bowl volume (cm^3)	19.29
Dead volume (cm^3)	25.1
Connecting rod length (cm)	16
Injector aperture No.	6
Fuel injection nozzle diameter	0.149
Nozzle injection angle	154
Fuel type	Diesel #2
Injection fuel temperature	285

The overall amount of soot and HC pollutants was evaluated prior to outlet valve opening. Different fuel injection gestures and timetables may strongly affect pollutant formation; hence, a multi-step injection strategy and retarded injection times were experimented and their effectivity on pollutant formation was investigated.

First, amount and procedure of HC and soot pollutant formation in crevice volumes inside the chamber under normal diesel engine conditions was studied in this article and then it was tried to prevent their formation by use of a multi-step injection method. Under normal conditions, only a single injection with trapezoidal configuration was available which its timetable was 2 degrees before top dead center and 2 degrees after top dead center in advance mode while it was6 degrees before top dead center in retarded mode.

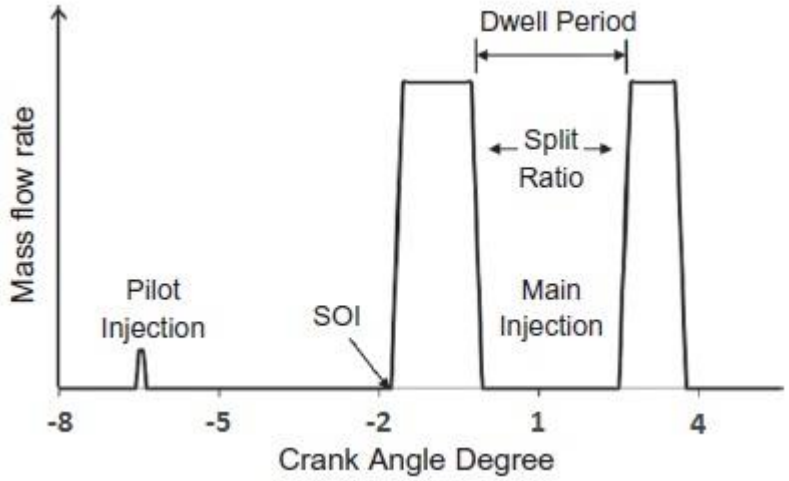

Figure 3. Fuel injection configuration.

Table 5. Engine operation and fuel injection configurationconditions.

	Case 1	Case 2	Case 3	Case 4	Case 5	Case 6
Start of injection	-6	-2	+2	-6	-6	+2
Injection configuration	Single injection	Single injection	Single injection	75/0/25	60/0/40	60/0/40
Overall injected fuel (mg)	25.4	26.4	27.6	25.6	25.3	26.7
Pilot fuel injection (mg)	0	0	0	0.521	0.521	0.521
Equivalence ratio	0.707	0.734	0.768	0.679	0.671	0.708
Inlet pressure (bar)	1.01	1.01	1.01	1.06	1.06	1.06
Inlet air temperature (°K)	313	313	313	313	313	313

Under multi-step injection conditions, fuel injection configuration consisted of a pilot fuelinjectionthat 5 degrees after which main injection was carried out. Fuel mass flow was divided into two pulses for the main fuel injection. Mass flow of these pulses was in 75/25 and 60/40 proportions so that a constant injection period with zero mass flow was considered. Figure 3 shows a schema of fuel injection. Experiment steps based on fuel injection is given in Table 5.

3-1- Verification

The experimental results obtained from this engine by Tan et al. were compared with simulation results from AVL Fire. Experimental data conditions are given in Table 6 and comparison results are illustrated in figures 4 and 5.

Table 6. Experimental conditions to compare theoretical and experimental results.

	Test 1	Test 2
Start of injection	-10	-5
Injection configuration	Single injection	Single injection
Overall injected fuel (mg)	30	28

Equivalence ratio	0.78	0.72
Inlet pressure (bar)	1.5	1.5
Inlet air temperature (°K)	300	300

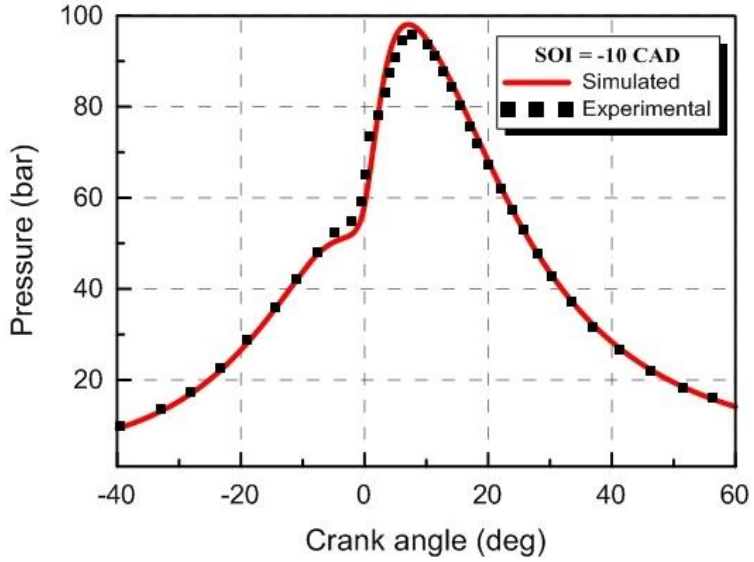

Figure 4. A comparison between theoretical and experimental results at 10 BTDC.

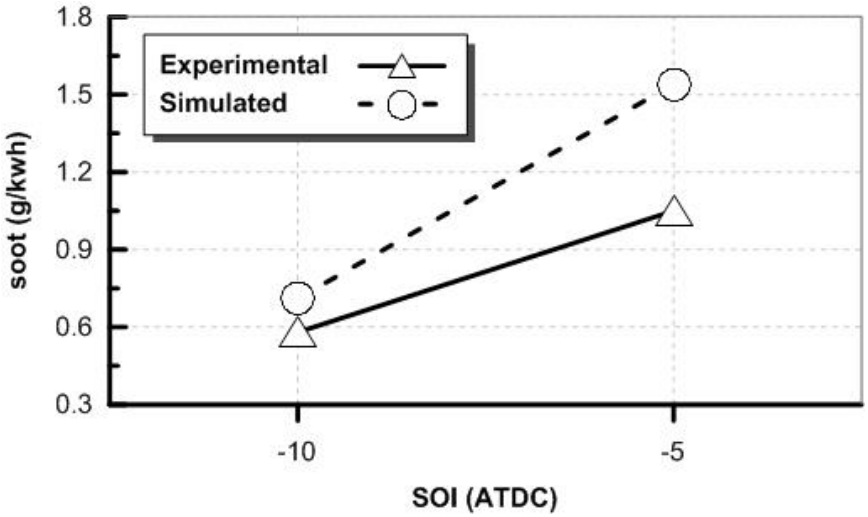

Figure 5. A comparison between theoretical and experimental results of soot pollutant.

4. RESULTS AND DISCUSSION

4.1. Contours combustion and emissions

Chamber contours at a two-stepinjection mode is shown in Figure 6. Right-hand contours imply reaction progress. 75 per cents of fuel was injected in the first step while the rest was injected in the second one; therefore, major combustion process occurred before top dead center and it ended after the second step of fuel injection.

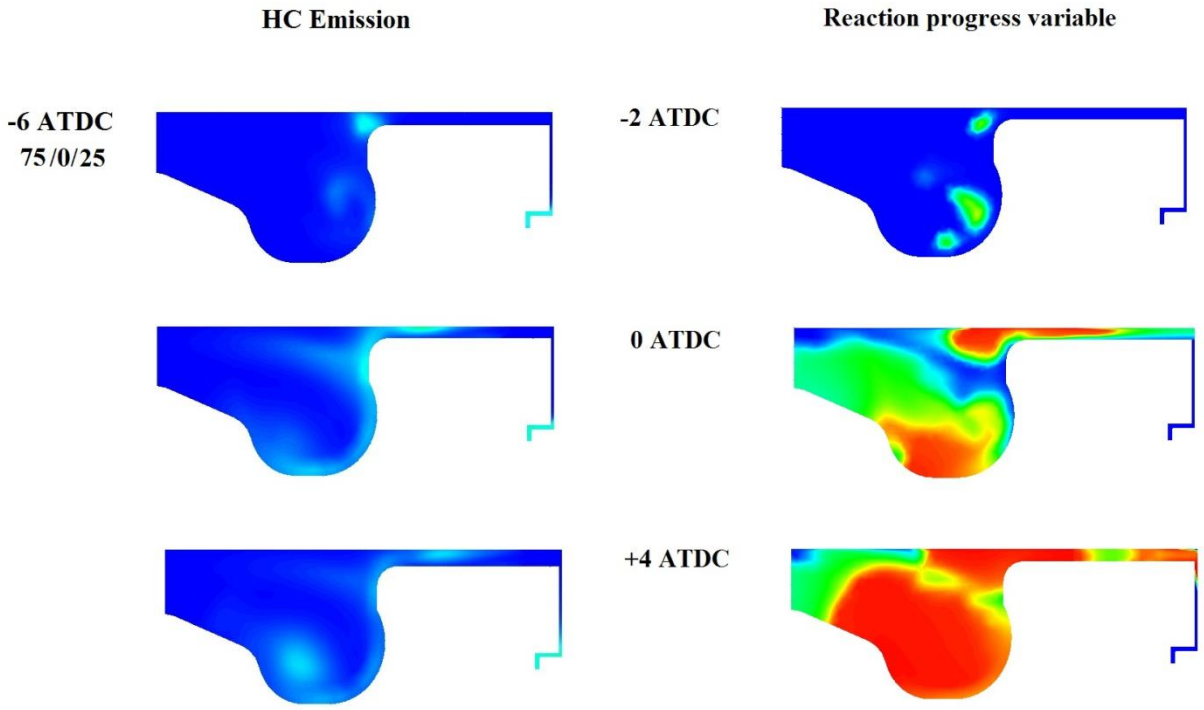

Figure 6. HC contours (left) and flame propagation (right) in a two-step injection mode at 25/0/75, 6 degrees before top dead center.

Hence, most hydrocarbons were oxidized by two steps of combustion. As it may be observed in Figure 6, flame fills chamber except the crevices; however, fuel does not accumulate in such areas due to two-step nature of fuel injection. In addition, few hydrocarbons were formed in both piston bowl and crevices.

The two-step fuel injection with 60 to 40 at -6 and +2 degrees after top dead center is illustrated in Figure 7. Increasing the volume of fuel injected in the second stepsignificantly prompted HC formation in the center of cylinder yet lessened them in crevices. Fuel injection at 2 degrees after top dead center would maximize HC pollutant amount with almost no fuel accumulation in crevices.

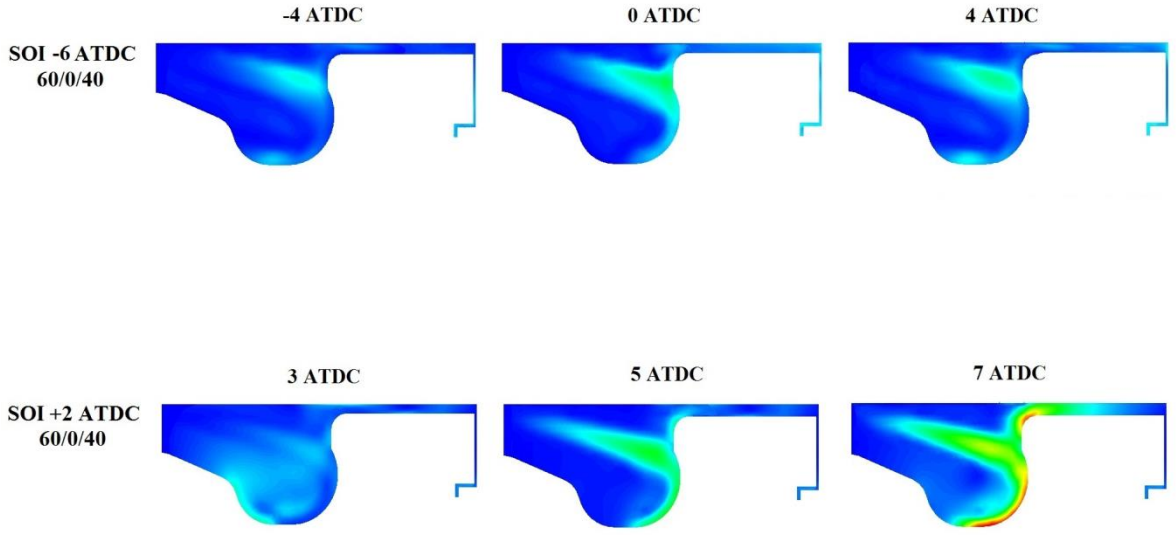

Figure 7. HC pollutant formation contours in a two-step injection mode at 40/0/60, -6 and +2 degrees after top dead center.

4.2. Primary results and curves of combustion

Figure 8 shows average temperature inside the chamber and released energy implying the fact that the more remained hydrocarbons led to decrease in released energy and average temperature. Lack of energy may cause incomplete combustion and reduction of engine power.

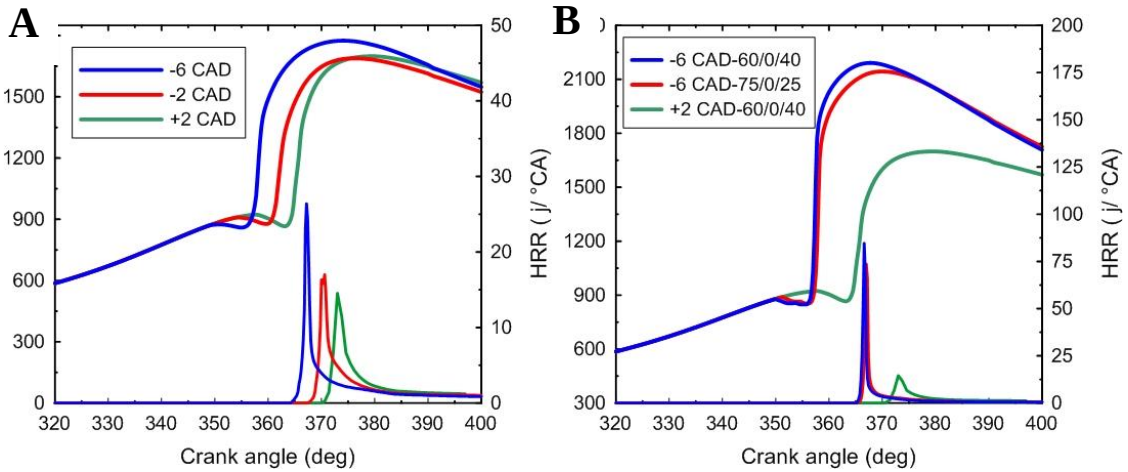

Figure 8. Average temperature of cylinder and released heat at single (A) and two-step (B) injection.

Engine power at different fuel injection modes is shown in Figure 9. It was observed from released heat curves that combustion intensity increased in two-step fuel injection mode. Combustion intensity itself leads to more engine power. However, in all cases, retarding fuel injection led to decrease in engine power because pressure peak and effective work decline after combustion.

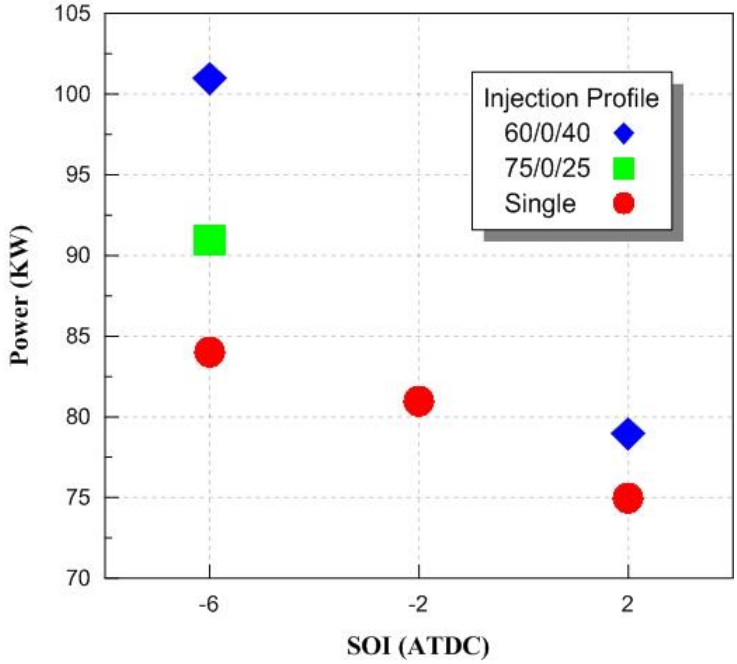

Figure 9. Gross engine power at different fuel injection modes.

Soot pollutant formation rate from the beginning to opening of outlet valve is shown in Figure 10.This pollutant grows negatively and diminishes at the two-step mode which is due to the second combustion step and burning of carbon particles. Soot formation continued up to the final moment and kept increasing at the single injection mode, 6 degrees before top dead center. Due to default settings of chemical kinetics for the software, the produced eddies react with fuel in the

chamber and reaction continues unless eddy production stopped. As a result, residuals either would remain as hydrocarbons or form soot as carbon pollutants.

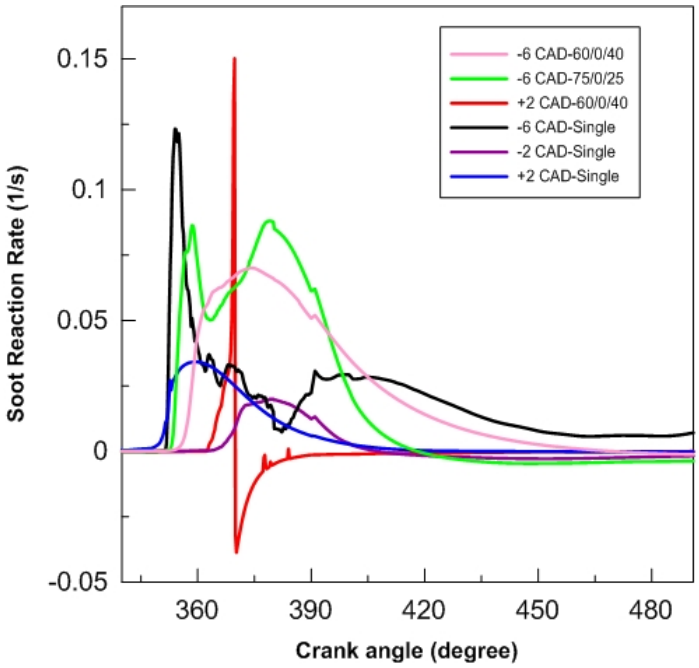

Figure 10. Soot formation rate at different fuel injection modes.

4.3. Pollutants

Pollutant distribution (g/kWh) is shown in Figure 11. Complete combustion and burn of components inside the chamber occurs during the two steps which is why HC and CO pollutants at this injection mode, 6 degrees before top dead center were formed in minimum amount. At 2 degrees after top dead center, HC and soot pollutants were high and CO was also increased because of incomplete combustion in such cases. Formation of NO_x, highly dependent on the average cylinder temperature, was positively affected by combustion intensity and temperature increase. As it may be seen in Figure 8, combustion intensity and average temperature at the two-step injection was more than 1800 °K and NO_x amount was expected to increase.

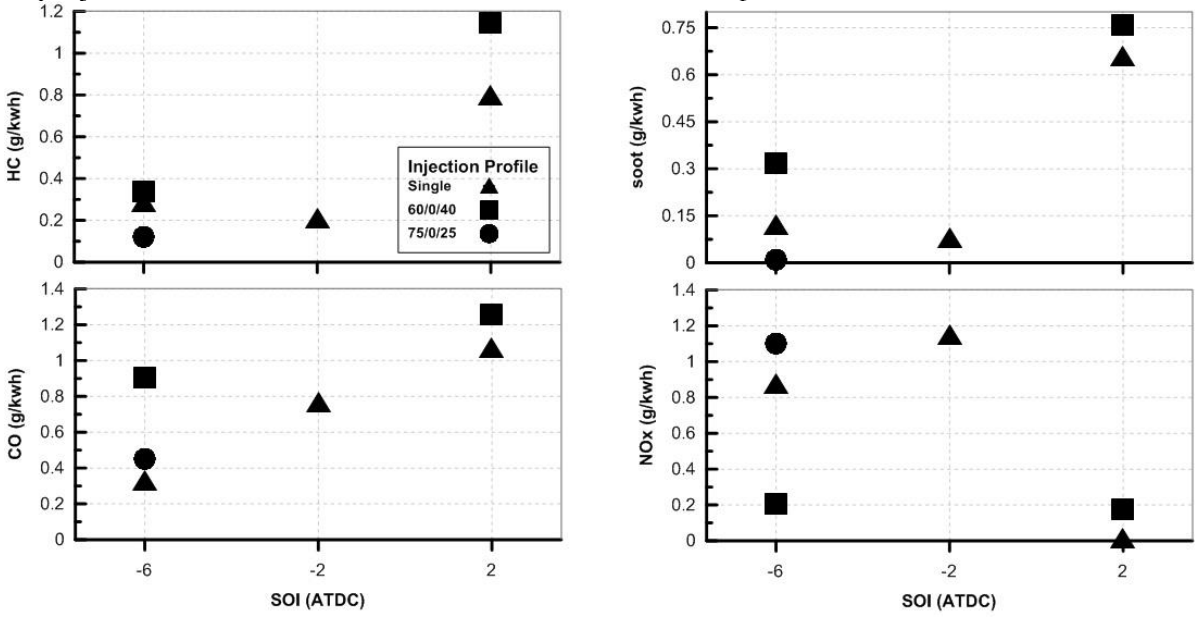

Figure 11. Calculated amounts of pollutants at different fuel injection modes.

4.4. The effect of crevices inside the chamber on the obtained results

The formed pollutants through both models are shown in Figure 12. It is clear that most of HC and soot pollutants formed within the crevice volumes. The model without crevice and liner showed less soot and HC pollutant.

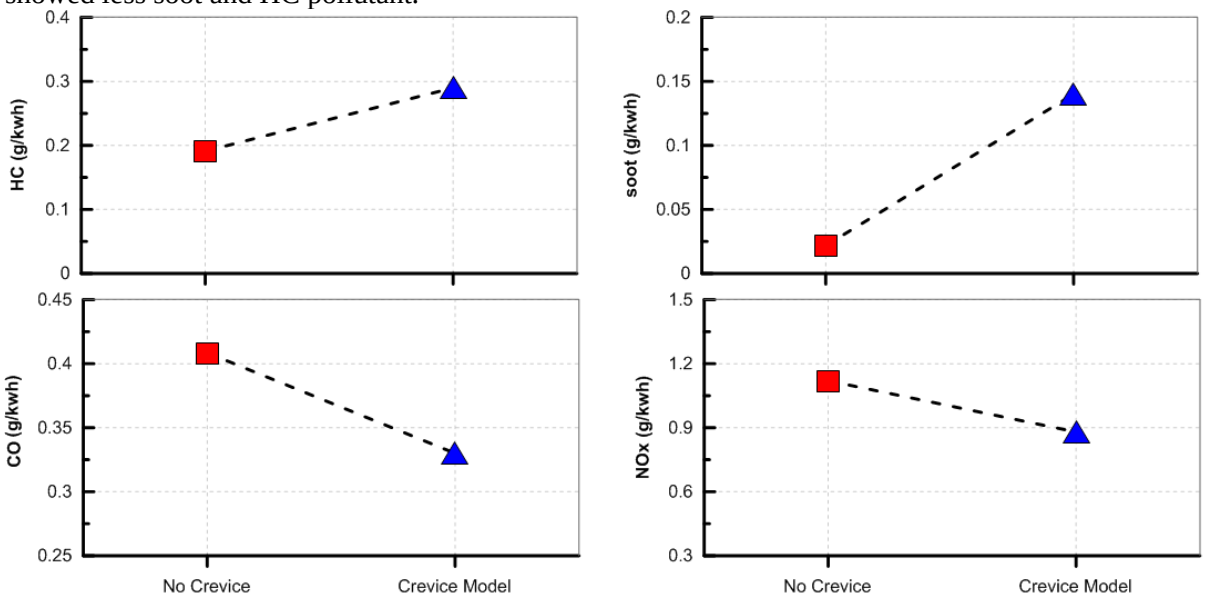

Figure 12. A comparison between crevice-bearing and crevice-free models.

On the other hand, CO had a considerably high amount in crevice-free model. CO is low in diesel engines due to dilution of the fuel; thus, fuel concentration and CO increase when crevices in the cylinder are taken into account. In the case of NO_x, more intensified combustions and higher cylinder temperatures led to increase in NO_x amount. High NO_x amount here also implies on this matter.

5. CONCLUSION

In the present work, the effect of various parameters on formation of HC pollutants (unburned hydrocarbons) which occurs due to their transition into grooves and crevices of the combustion engine in a light diesel engine was investigated.Numerical calculations for simulation of the combustion chamber were carried out by means of AVL Fire software.The effects of crevices and regions among the wall and the cylinder on formation of HC pollutants under different fuel injection methods at basic diesel engines were studied. Single-injection at different times as well as various fuel amounts formed the fuel injection configuration. The following conclusions may be made:

1- Increasing the volume of fuel injected in the second step significantly prompted HC formation in the center of cylinder yet lessened them in crevices.
2- The more remained hydrocarbons lead to decease in released energy and average temperature. Decrease in released energy may bring about other consequences such as incomplete combustion and reduction of engine power.
3- Soot formation continued up to the final moment and kept increasing at the single injection mode, 6 degrees before top dead center. However, this pollutant grows negatively and diminishes at the two-step mode.

4- At 2 degrees after top dead center, HC and soot pollutants were high and CO was also increased because of incomplete combustion in such cases. Formation of NO_x, highly dependent on the average cylinder temperature, was positively affected by combustion intensity and temperature increase.

5- The model without crevice and liner showed less soot and HC pollutant. CO had a considerably high amount in crevice-free model. Besides, themore intensified combustions and higher cylinder temperatures led to increase in NO_x amount.

REFERENCES

[1] R.B. Krieger and G.L. Borman. The computation of apparent heat release for internal combustion engines. ASME, 1967.

[2] W.T. Lyn. The spectrum of diesel combustion research. Proc. Inst. Mech. Engrs., 184 (3J) (1969–1970), pp. 1–15

[3] G. A. Karim and H. C. Watson "Experimental and Analytical Examination of the Development of Inhomogeneities and Autoignition During Rapid Compression of Hydrogen-Oxygen-Argon Mixtures". J. Eng. Gas Turbines Power125(2), 458-465 (Apr 29, 2003)

[4] Karim, G.A. and Gao, J. 1992, A Predictive Model for Knock in Gas Fuelled Spark Ignition Engines, SAE. Paper no. 922366

[5] G. A., Karim, and Y., Zhaoda, "Modeling of Auto -Ignition and Knock in a Compression Ignition Engine of the Dual Fuel Type", IMechE (Institution of Mechanical Engineering), C430/033, (1991), l41-148.

[6] Z., Liu and G. A., Karim, "A Predictive Model for the Combustion Process in Dual Fuel Engines", SAE Paper,No. 952435, (1995).

[7] Hiroyasu, H. and Arai, M. "Structures of Fuel Sprays in Diesel Engines", SAE 900475.

[8] H.Hiroyasu, T.co-workers , Fuel Spray Characterization in Diesel Engines, in Combustion Modelin in Reciprocating Engines (edited by Mattavi J. N. and Amann C. A.,Plenum Press), pp.369-408,1980

[9] A.P. Watkins "A contribution to the design of a novel direct- injection diesel engine combustion system analysis of pip size Applied Mathematical Modelling, 17 (3) (1993), pp. 114–124

[10] Jones WP, Launder BE (1972) The Prediction of Laminarization with a Two-Equation Model of Turbulence. Int J Heat and Mass Transfer, vol 15, p 301

[11] Butler, S., " A Predictive Model forKnock in Dual Fuel Engines", Transactions of SAE,SAE (Society of Automotive Engineering) Paper, No.921550, (1992).

[12] C., Mansour, A., Bounif, A., Aris and F., Gaillard, "Gas- Diesel (Dual - Fuel) Modeling in Diesel Engine Environment", Int. J. Therm. Sci., Vol. 40, (2001), 409-424.

[13] AVL Manual "CFD-Solver_v2010_04_ICE-Physics-Chemistry"

[14] Bockhorn, H. ed. "Soot Formation in Combustion: Mechanisms and Models.",Springer, 1994.

[15] J. Warnatz · U. Maas · R.W. Dibble," Combustion Physical and Chemical Fundamentals, Modeling and Simulation, Experiments, Pollutant Formation," 4th Edition.2006.

[16] Hiroyasu, H., and Nishida, K. "Simplified Three Dimensional Modeling of Mixture Formation and Combustion in a DI Diesel Engine." SAE 890269, 1989.

[17] S.M. Tan, H.K. Ng, S. Gan. Computational study of crevice soot entrainment in a diesel engine. Applied Energy 102: 898-907, 2013.